Observation of Self-Trapping of an Optical Beam Due to the Photorefractive Effect

Galen C. Duree, Jr., John L. Shultz, and Gregory J. Salamo
Department of Physics, University of Arkansas, Fayetteville, Arkansas 72701

Mordechai Segev and Amnon Yariv
California Institute of Technology, Department of Applied Physics, Pasadena, California 91125

Bruno Crosignani and Paolo Di Porto
Dipartimento di Fisica, Università dell'Aquila, L'Aquila, Italy and Fondazione Ugo Bordoni, Roma, Italy

Edward J. Sharp
Army Research Laboratory, Fort Belvoir, Virginia 22060

Ratnakar R. Neurgaonkar
Rockwell International Science Center, Thousand Oaks, California 91360
(Received 19 April 1993)

We report on the first observation of self-trapping of an optical beam due to the photorefractive effect. The self-trapping occurs at microwatt light power levels, is intensity independent, and results in significant spatial pulse reshaping.

PACS numbers: 42.65.Jx, 42.50.Rh, 42.65.Hw

Self-trapping of laser beams in nonlinear Kerr media is a well studied phenomenon [1–6] in which the diffraction effects are exactly compensated by focusing effects caused by a light induced index change. In these cases, the propagation of a light beam is spatially confined and a shape-preserving transverse profile or spatial soliton is observed. Recently, a new type of spatial soliton has been suggested [7]. It has been predicted to occur in a photorefractive medium and differs from Kerr solitons by the fact that the focusing effect is produced by an internal nonlocal space-charge dc field, as opposed to the local intensity dependent Kerr effect. A dramatic consequence of the difference in the focusing origin is that the photorefractive soliton is observable at low light powers on the order of 10 μW (intensities of about 200 mW/cm^2) or less while the observation of "bright" [5] or "dark" [6] Kerr solitons requires much higher powers. Moreover, photorefractive solitons are independent of the laser light power. As a result, they propagate while maintaining their spatial profile even in the presence of loss or gain.

In this Letter, we report the observation of photorefractive solitons. These solitons preserve their profile, which are independent of input power, and can be observed at low light powers of less than 10 μW. The degree of self-focusing due to the photorefractive index change is shown to be controllable by an applied dc voltage across the photorefractive crystal. For small applied voltages, diffraction is seen to exceed the photorefractive focusing effect and the transmitted beam is observed to diverge through the crystal. For large applied voltages, the photorefractive focusing effect exceeds diffraction and the transmitted beam is observed to converge throughout the crystal. Only for a small range of applied voltages is a shape-preserving spatial profile observed to propagate throughout the crystal. This voltage range has been predicted in Ref. [7] and is dictated by the crystal parameters, such as its electro-optic coefficients, the dielectric constant, the density of traps, and the light wavelength and polarization. For very large applied voltages, photorefractive focusing greatly exceeds diffraction and the incident beam converges in the crystal to a spot size smaller than its original waist. Following the formation of the new waist, the beam diverges and is then trapped as diffraction is once again compensated for by the focusing produced via photorefraction. In all cases, the laser beam is observed to reshape and take on a "smooth" spatial profile.

For photorefractive solitons the photorefractively induced change in the index of refraction of the medium can be thought of as arising from the photorefractive two-wave mixing between all possible pairs of the plane-wave spatial-frequency spectrum of the incident laser beam [7,8]. That is, for each pair of plane-wave components of the incident beam which interferes and produces an interference grating throughout the crystal, a perturbation in the refractive index is generated $\delta n(r,z)$, where z is along the propagation direction and r is in the plane perpendicular to z. Each corresponding index grating may be viewed as a composition of two grating components: One is in phase, spatially, with the original interference pattern and the other is 90° out of phase. The in-phase component is responsible for phase coupling between the plane waves, and therefore can compensate for diffraction while the 90° phase shift component is responsible for energy exchange between each pair of spatial-frequency plane-wave components of the incident beam and for stimulated scattering or "beam fanning" [9,10]. In order to generate a nondiffracting light beam, we require $\delta n(r,z)=\delta n(-r,z)$, for all z, since diffraction is symmetric about the z axis. Following the discussion in Ref. [7] on the symmetry properties of the coupling coefficient, $\hat{\delta n}$ in the simple scalar 2D case, we have used

the experimental configuration suggested there. However, in this configuration, where the light propagates perpendicular to the optic axis (c axis) and a voltage is applied along the c axis, the energy-exchange process is asymmetric about the direction of propagation, and may deteriorate the shape-preserving propagation. For most of the experimental results reported here, we used external fields E_0 in the range $E_d \ll |E_0| \ll E_p$ (as suggested in Ref. [7] where E_p is the limiting space-charge field and E_d is the diffusion field) in order to minimize the out-of-phase component of the index grating and hence energy-exchange effects. Meanwhile, the relative magnitude of the in-phase gratings must be controllable in order to compensate for diffraction. This was accomplished by adjusting the value of an applied dc electric field, and by proper choice of the transverse profile of the incident light beam. For example, soliton solutions include the hyperbolic-secant and Gaussian spatial shape-preserving profiles. These solutions exist for applied fields in a range calculated using the appropriate experimental and crystal parameters in the expression given in Ref. [7].

The basic apparatus consisted of a cw argon-ion laser and a 5 mm×5 mm×6 mm strontium barium niobate (SBN) crystal with 0.01% by weight rhodium dopant. The cw argon-ion laser wavelength was 457 nm and its output beam diameter was 1.5 mm. A schematic diagram of the apparatus is shown in Fig. 1. The output beam was directed onto a 10 cm focal length lens and the SBN crystal was placed 3.6 mm beyond the beam waist of $2\omega_0 = 33$ μm. The beam diameter at the SBN crystal entrance face was 71 μm in the vertical plane and 81 μm in the horizontal plane. The crystal was oriented with its c axis in the horizontal plane and perpendicular to the propagation direction of the incoming laser light. The polarization of the incoming light could be varied using a polarization rotator but was initially chosen to be along the c axis (extraordinary polarization). The beam diameter throughout the crystal was measured using an imaging system consisting of an imaging lens, L_2, and a two-dimensional detector array. The input face of the 6 mm long SBN crystal was well beyond the Rayleigh range of 1.5 mm from the beam waist formed by the focusing lens, L_1. The imaging system, therefore, imaged the beam spot at the SBN entrance face with some magnification onto the detector array. As the imaging lens and the detector array are moved away from the SBN crystal, different cross sections of the Gaussian beam are then imaged onto the array. In this manner, the beam diameter at different locations throughout the SBN crystal was monitored. The magnification of the imaging system was determined by placing a thin aperture on the crystal exit (and entrance) face and imaging the aperture onto the detector array. Using the known value of the reference aperture, the magnification was determined to be about 15 and the positions of the exit and entrance faces of the SBN crystal were located. Using this information the horizontal cross section of the incident beam on the entrance and exit faces of the crystal was determined and is shown in Figs. 2(a) and 2(b).

A potentially serious problem in the observation of the photorefractive soliton is the interaction of the light beam with scattered light. The scattered light is amplified toward a preferential direction (given by the symmetry properties of the energy-exchange coupling coefficient, or the imaginary part of δn), and transforms the input beam into a broad fan of light. This "fanning" appears in most photorefractive crystals with nonzero energy-exchange coupling. We minimized the fanning effects by using a focused beam inside the crystal [9]. In fact with zero applied field no noticeable beam fanning was observed. Even with the applied voltage of 400 V/cm, which was

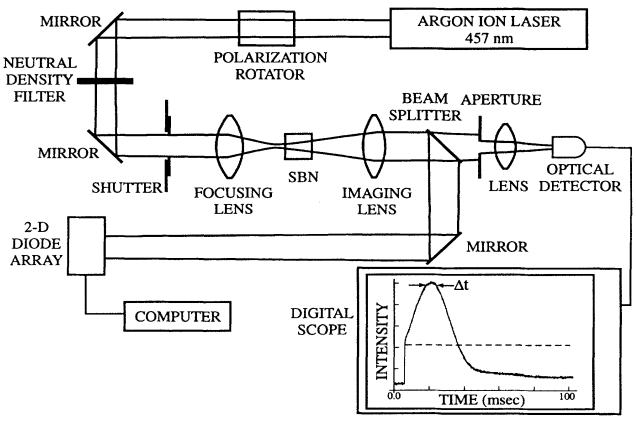

FIG. 1. Experimental apparatus used to observe photorefractive solitons.

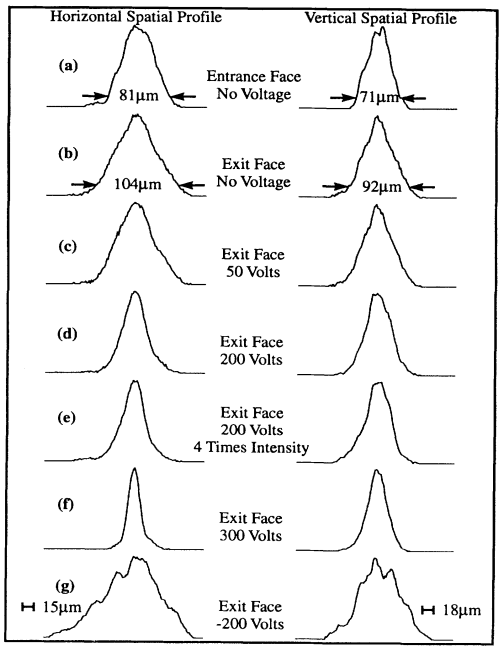

FIG. 2. The horizontal and vertical spatial beam profiles are shown for various applied voltages.

needed to observe soliton formation, beam fanning was observed to be a small effect. This was true for two reasons. First, the resulting small beam diameter provides small gain length to interactions with noise in directions that deviate significantly from $\hat{z}$ due to small interaction lengths. Second, for directions at small angles to $\hat{z}$, where large interaction lengths are possible, the gain length is again small due to small gains at the low voltage of 400 V/cm. In all directions, therefore, at voltages of 400 V/cm the gain-length product was small and beam fanning was correspondingly weak. Moreover, given that the gain length was small and the intensity modulation also small (due to the low intensity of the scattered light) the fanning which was observed was seen to form at times much longer [10,11] than the time for soliton formation. This means that for the experiment reported here, at applied voltages of 400 V/cm, soliton formation reached equilibrium before beam fanning effects needed to be considered. Consequently, a direct comparison between theory and experiment is possible. Therefore, experimentally we observed the propagating spatial profile early in time, before any beam fanning took place. This observation region is referred to as the "steady-state" region since the propagating spatial profile remained constant during this time period. This period was determined by monitoring the intensity of the incident beam after passing through the crystal and an exit aperture which was adjusted to be about the size of the incident beam. The transmission data indicated that self-focusing took place before fanning could be observed. The inset in Fig. 1 shows the total energy transmitted through the aperture as a function of time. Without an applied voltage, no self-focusing or beam fanning effects were observed (dashed curve). When self-focusing effects occurred (after applying an external dc voltage), the transmitted energy first increased, reached a steady state, and then diminished for large times (solid curve) due to screening of the applied field in the case of low applied voltages and both beam fanning and screening for large applied voltages. The steady-state region provided a window in time when diffraction effects (or solitons) could be observed with very little fanning present. For a voltage of 50 V (or an electric field of 100 V/cm) applied along the **c** axis, the spatial profile and beam diameter at the plane containing the crystal is shown in Fig. 2(c). The figure indicates that the beam is diverging as it propagates from the entrance face to the exit face. Comparing Fig. 2(b) to Fig. 2(c), however, it is evident that the divergence experienced by the beam along the **c** direction in propagating through the crystal is less with an applied field. Increasing the applied voltage to 300 V or an applied field of 600 V/cm, we can see in Fig. 2(f) that the beam now converges as it propagates through the SBN crystal. Apparently the photorefractive focusing produced with 50 V is not sufficient to compensate for diffraction while the focusing produced for 300 V overcompensates. Figure 3 shows the beam diameter and spatial profile of the laser

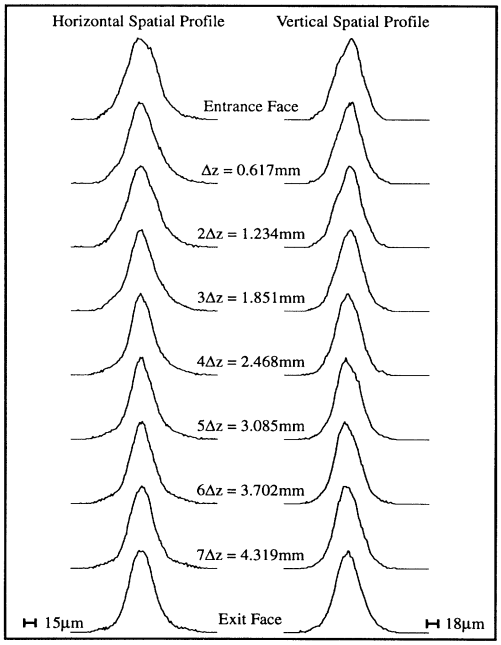

FIG. 3. Spatial beam profiles inside the crystal with 200 V.

beam propagating through the crystal with 200 V or a field of 400 V/cm applied. In this case, the beam diameter and spatial profile are observed to remain nearly constant as it propagates through the crystal and can be described as a photorefractive spatial soliton. The temporal window or steady-state region for this measurement was at least 130 msec. Experimentally, therefore, we have observed the formation of a shape-preserving propagating beam with an applied voltage in the range of 400 to 500 V/cm across the crystal. Theoretical prediction, using the parameters for our particular SBN:60 rhodium doped crystal, is also in the range of 400 to 500 V/cm. For the very large field case, $V = 3000$ V, Fig. 4 shows the beam diameter and spatial profile of the laser beam propagating through the crystal. In this case, a smooth spatial profile is more apparent. In both high and low voltage cases, a spatial soliton appears to have formed along both the **c** direction and the direction perpendicular to **c** (but with different cross section). The immediate consequence is that a soliton was formed in both transverse dimensions, a capability that was until now restricted to dark soliton stripes and grids [6]. In fact, this is the first observation, to our knowledge, of any two-dimensional bright soliton. From the temporal evolution of this high voltage soliton we infer that the perturbation in the index did *not* reach its steady state at the time at which we made the trapped-profile measurement. Unlike all other cases, where the temporal evolution had a flat, steady-state region, this high voltage case always had a temporal gradient: first due to the evolution of the soliton, then due to its breakdown (when the value of the index change exceeds the soliton upper limit), and finally due to the evolution of fanning. We have used a narrow temporal

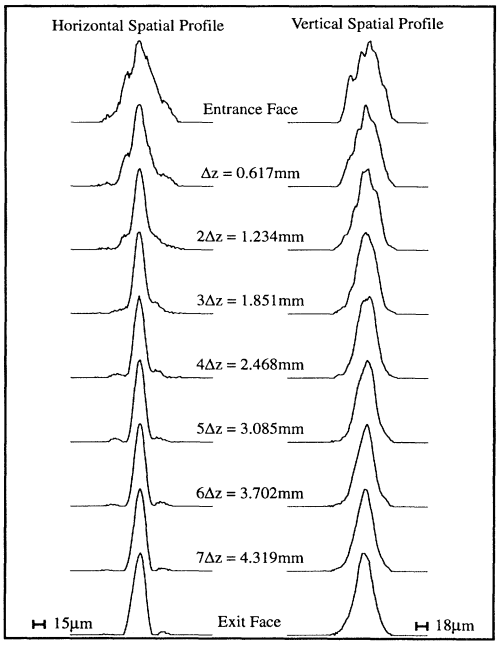

FIG. 4. Spatial beam profiles inside the crystal with 3000 V.

window of about 4 msec in this case. However, the temporal curve had a significant gradient even within this window, which indicates that the index change never reached a steady state before evolution of fanning.

In addition to comparing theory and experiment for the applied voltage range for which soliton formation is observed and predicted we also compared theory and experiment for the parameters of incident light polarization, incident light intensity, the polarity of the applied voltage, and the transverse phase of the photorefractive soliton. For example, when the polarization of the incident laser light was changed to be perpendicular to the c axis, the voltage necessary to compensate for diffraction was experimentally estimated to be about 500 to 600 V or an electric field of 1000 to 1200 V/cm. This would suggest, according to the derivation in Ref. [7], that r_{33} is an order of magnitude larger than r_{13}. This difference is consistent with published reports of this ratio. We also observed that with ordinary polarization the beam fanning appeared only after about 1 sec and was minimal during the temporal window of the measurement.

When the incident intensity was increased by a factor of 4, we observed that both the beam diameter and spatial profile were unchanged in full support of the prediction that photorefractive spatial solitons would form and be independent of the incident intensity. This is demonstrated in Figs. 2(d) and 2(e). Also, to be sure that the observed soliton propagation or formation was indeed photorefractive in origin, we intentionally interrupted the writing of the phase gratings and observed that they remained in the crystal for days but could be immediately erased with an incoherent intense light source.

Finally, when the polarity of the dc voltage was reversed, no soliton was observed. This can be explained by the sign of the in-phase part of the index grating, which causes the input beam to diverge. Intuitively, the self-generated positive lens turns into a negative self-generated lens, and increases diffraction. This is shown in Fig. 2(g). Again, these results are in full agreement with theoretical predictions.

Another issue is the transverse phase of the photorefractive soliton. In Ref. [7] it was assumed, rather than proved, that the transverse phase of the soliton is uniform. We have experimentally verified that this is the case by examining the diffraction or propagation of the exiting light beam using our imaging system. In particular, the beam exiting the crystal is observed to propagate while maintaining a smooth near Gaussian shape. Moreover, the beam diameter at the crystal exit face is seen to play the role of "minimum waist" for the beam propagating from the exit face. We have in fact recently proven theoretically that all soliton solutions possess uniform transverse phase.

Following these experimental observations, we have succeeded in showing theoretically and experimentally that the photorefractive solitons are stable in the presence of small perturbations, but break down in the case of large perturbations. The stability is manifested in the work presented here through the reshaping and the shape-preserving profiles of the solitons, *despite* the material inhomogeneities that cause the profile perturbation seen in Figs. 2(a) and 2(b).

In conclusion, we report the first observation of photorefractive spatial solitons. These observations are in full agreement with earlier theoretical predictions.

[1] R. Y. Chiao, E. Garmire, and C. H. Townes, Phys. Rev. Lett. **13**, 479 (1964).
[2] V. E. Zakharov and A. B. Shabat, Zh. Eksp. Teor. Fiz. **61**, 118 (1971) [Sov. Phys. JETP **34**, 62 (1972)].
[3] J. E. Bjorkholm and A. Ashkin, Phys. Rev. Lett. **32**, 129 (1974).
[4] A. Barthelemy, S. Maneuf, and C. Froehly, Opt. Commun. **55**, 201 (1985).
[5] J. S. Aitchison, A. M. Weiner, Y. Silberberg, M. K. Oliver, J. L. Jackel, D. E. Leaird, E. M. Vogel, and P. W. Smith, Opt. Lett. **15**, 471 (1990).
[6] G. A. Swartzlander, D. A. Andersen, Y. Y. Regan, H. Yin, and A. J. Kaplan, Phys. Rev. Lett. **66**, 1583 (1988).
[7] M. Segev, B. Crosignani, A. Yariv, and B. Fischer, Phys. Rev. Lett. **68**, 923 (1992); B. Crosignani, M. Segev, D. Engin, P. DiPorto, A. Yariv, and G. Salamo, J. Opt. Soc. Am. B **10**, 446 (1993).
[8] M. Segev and A. Yariv, Opt. Lett. **16**, 1938 (1991).
[9] M. Segev, Y. Ophir, and B. Fischer, Opt. Commun. **77**, 265 (1990).
[10] M. Segev, D. Engin, A. Yariv, and G. C. Valley, Opt. Lett. **18**, 956 (1993).
[11] H. Rajbenbach, A. Delboulbé, and J. P. Huignard, Opt. Lett. **14**, 1275 (1989).